

# Dynamic Light Scattering from Ternary Solutions of Semiflexible Polymers

Paul S. Russo

Macromolecular Studies Group, Department of Chemistry, Louisiana State University, Baton Rouge, Louisiana 70803-1804. Received March 26, 1985

**ABSTRACT:** Dynamic light scattering has been used to study ternary polymer solutions of the type long semiflexible rod/short semiflexible rod/solvent. The semiflexible rods are helical poly( $\gamma$ -benzyl  $\alpha$ -L-glutamate). The correlation functions are well fit by two exponentials. The slow mode, corresponding to diffusion of the dilute longer rod, decreases to as little as 20% of its dilute binary solution value as concentration of the shorter rods is raised. Although the details of the decrease are not thoroughly clear, its magnitude is comparable to that seen earlier in concentrated binary solutions of poly( $\gamma$ -benzyl  $\alpha$ -L-glutamate), where a thermodynamic correlation is required (Russo, P. S.; Langley, K. H.; Karasz, F. E. *J. Chem. Phys.* 1984, 80, 5312), but much smaller than that reported recently in concentrated binary solutions poly(*n*-butyl isocyanate) in  $\text{CCl}_4$  (Statman, D.; Chu, B. *Macromolecules* 1984, 17, 1537) after an entirely different analysis. These results are discussed in terms of rod flexibility.

## Introduction

The true self-diffusion coefficient,  $D_{\text{self}}$ , of the semiflexible polymer poly( $\gamma$ -benzyl  $\alpha$ -L-glutamate) (PBLG) dissolved in the good solvent *N,N*-dimethylformamide (DMF) was recently estimated by applying a thermodynamic correction factor to the mutual diffusion coefficient measured in dynamic light scattering and assuming equal friction factors  $f_{\text{self}} = f_{\text{mutual}}$ .<sup>1</sup> As the concentration was raised, the estimated self-diffusion coefficient,  $D^I$ , decreased to less than  $0.5D^\circ$  where  $D^\circ$  is the diffusion coefficient at zero concentration and  $0.5D^\circ$  represents the Doi-Edwards expectation in the semidilute regime.<sup>2,3</sup> If  $N$  is the number density of rigid rods with length  $L$  and diameter  $d$ , this region is bounded by

$$L^{-3} \ll N \ll L^{-2}d^{-1} \quad (1)$$

The Doi-Edwards expectations for  $D_{\text{self}}$  and the rotational diffusion constant,  $\Theta$ , are respectively

$$D_{\text{self}} = D^\circ/2 = D_{\parallel}^\circ \quad (2)$$

$$\Theta = \beta\Theta^\circ/(NL^3)^2; \quad \beta \simeq \text{order } (1-10) \quad (3)$$

Superscript  $^\circ$  represents the infinitely dilute limit. Equation 2 is obtained by assuming that diffusion perpendicular to the rod axis,  $D_{\perp}$ , is 0, while diffusion parallel to the rod axis,  $D_{\parallel}$ , is unhindered. This should be reasonable not only for binary solutions of rodlike polymers but also for ternary solutions in which a thin rodlike polymer moves through a constraining matrix. In eq 3,  $\beta^{1/2}$  may be viewed as the value of  $NL^3$  at the onset of entanglement of the rods. By a rather indirect argument, it was estimated that  $\beta^{1/2} \simeq 20$ .<sup>1</sup> Though surprisingly large, this is among the smallest values in the literature.<sup>3-10</sup> The delayed onset of entanglement was explained by an escapement mechanism arising from minor flexural motions of the imperfectly rigid rods, although the size and structure of the entanglement "cage" is also an important factor.<sup>8</sup> Together with their finite thickness, the flexibility of the rods was also hypothesized to account for the reduction of  $D^I$  to values lower than  $D^\circ/2$  by introducing barriers to motion parallel to the nominal axis, whereas no such barriers exist for the infinitely thin rigid rod. At very high concentrations, strikingly nonexponential correlation functions were measured. When an exponential sampling method<sup>11</sup> was used, these appeared to be bimodal, and the slow-mode decay rate appeared to scale as  $q$ , rather than as  $q^2$ , where  $q$  is the magnitude of the scattering vector. This is in qualitative agreement with the scattering correlation function predicted by Doi and Edwards,<sup>2a</sup>

which has a long time-decay rate proportional to the geometric mean of the rotational and diffusional decay rates.

Because of the finite cross section and imperfect rigidity of the molecules, it is not surprising that diffusion may be reduced below the  $D^\circ/2$  value expected from simple Doi-Edwards theory. However, there is considerable uncertainty as to precisely how much the self-diffusion is reduced. The extent of the reduction is the subject of this paper. Our previous result, based on an approximate thermodynamic correction, suggested reductions to perhaps  $D^\circ/8$  prior to liquid-crystal formation. The highest concentration in that study corresponds to  $NL^3 = 1500$  ( $NdL^2 = 15$ ). Zero and Pecora, who studied PBLG in dichloroethane, a thermodynamically poorer solvent than DMF,<sup>12</sup> found overall reductions of  $D$  to  $\simeq 2/3D^\circ$  without thermodynamic correction.<sup>4</sup> In contrast, the theory of Edwards and Evans,<sup>13</sup> which takes into consideration the finite cross section of perfectly rigid rods, yields a relationship, valid near  $N \simeq (dL^2)^{-1}$ , of the form

$$D_{\text{self}} = 0.5D^\circ(1 - g(NdL^2)^{3/2}); \quad g \simeq \text{order } (1) \quad (4)$$

Equation 4 predicts cessation of motion at some concentration that may or may not be achieved prior to formation of an anisotropic phase. Statman and Chu have applied the formalism underlying this equation to obtain a new expression for light-scattering correlation functions, which contains slow and fast decay modes, both proportional to  $q^2$ , even in the absence of translational-rotational coupling.<sup>14</sup> Identifying the average decay of the slow mode with  $D_{\text{self}} = D_{\parallel}$ , they find that  $D_{\parallel}$  is enormously reduced, even at relatively low concentrations, for the system poly(*n*-butyl isocyanate) (PBIC) in carbon tetrachloride. Their interpretation is summarized in Table I, and data from ref 1 are included for comparison. It is unclear whether differences in the systems studied or in the interpretation of data are responsible for the large differences represented in Table I. The PBIC fragment studied by Statman and Chu is probably shorter, relative to its persistence length,<sup>15</sup> than the PBLG sample of ref 1.<sup>16</sup> This might diminish the importance of escapement mechanisms, thereby enhancing entanglement effects. However, the origin of slow modes in concentrated binary polymer solutions, rodlike or otherwise, is still somewhat mysterious.<sup>17-20</sup> Accordingly, we have undertaken more direct (but still approximate) measurements of the self-diffusion of rodlike polymers in complex solution, using dynamic light scattering to observe the motion of relatively dilute rodlike

**Table I**  
Diffusion Data from Light Scattering in Two Binary Systems after Different Interpretations<sup>a</sup>

$NdL^2$	$NL^3$	$D_{  }^b \times 10^9$ cm <sup>2</sup> /s	$D_{  }/D^o$
0.55	44	5.29	0.038
0.97	76	3.14	0.022
1.08	87	2.71	0.020
1.45	117	1.96	0.014
1.70	137	1.46	0.010
2.48	200	0.72	0.0052
2.65	214	0.32	0.0022

$NdL^2$	$NL^3$	$D^I \times 10^7,^c$ cm <sup>2</sup> /s	$D^I/D^o$
0.022	2.23	1.30	0.98
0.146	15.0	1.15	0.86
0.217	22.3	1.12	0.84
0.292	30.0	1.04	0.78
0.437	44.9	0.94	0.71
0.583	59.9	0.83	0.62
0.729	78.9	0.73	0.55
2.51	258	0.40	0.30
3.90	400	0.34	0.26
7.41	761	0.25	0.19
14.7	1513	0.16	0.12

<sup>a</sup> At sufficiently high concentration,  $D^I$  should represent motions parallel to the rod axis,  $D_{||}$ . The Doi-Edwards prediction in this limit is  $D_{||} = D^o/2$ . <sup>b</sup> PBIC; as reported from average slow-mode decay in ref 14. Assuming  $L = 1212$  Å;  $d = 15$  Å,  $M = 75\,000$ . Persistence length for PBIC is uncertain, but the molecule appears to be rodlike up to  $M \approx 10^{5.15}$ . Error:  $\sim 10\%$ . <sup>c</sup> PBLG; as reported after thermodynamic correction in ref 1. Assuming  $L = 2055$  Å;  $d = 20$  Å,  $M = 300\,000$ . Persistence length for PBLG is quite uncertain<sup>16</sup> but  $\geq 700$  Å. Error:  $\sim 10\%$  below  $NdL^2 = 1$ ;  $\sim 20\%$  above  $NdL^2 = 1$ .

polymers (probes) in ternary solutions containing other polymers (the matrix) at much higher concentration. This paper gives some results for the simplest ternary system: long rod (probe)/short rod (matrix)/solvent. The system used is described in Table II.

### Theoretical Considerations

The light-scattering spectrum from a strongly interacting ternary solution has been considered by several authors.<sup>21-26</sup> The starting point in the theoretical developments<sup>21-23</sup> is the set of simultaneous diffusion equations describing the flux,  $J_i$ , of the polymeric components:

$$J_2 = -D_{22}\nabla c_2 - D_{23}\nabla c_3 \quad J_3 = -D_{32}\nabla c_2 - D_{33}\nabla c_3 \quad (5)$$

Here, 2 and 3 are labels for the two distinct polymer components, subscript 1 being reserved for the solvent;  $D_{22}$  and  $D_{33}$  are the diffusion coefficients associated with gradients in concentrations,  $c_2$  and  $c_3$ , of components 2 and 3, respectively;  $D_{23}$  is the cross-diffusion coefficient coupling fluxes of 2 to gradients in 3. It has been shown<sup>21-23</sup> that the correlation function of the electric field of light scattered by a system governed by these equations is

$$g^{(1)}(\tau) = A^+ e^{-\Gamma^+ \tau} + A^- e^{-\Gamma^- \tau} \quad (6)$$

where

$$\Gamma^\pm = \frac{1}{2} q^2 \{ (D_{22} + D_{33}) \pm [(D_{22} - D_{33})^2 + 4D_{23}D_{32}]^{1/2} \} \quad (7)$$

The coefficients  $A^+$  and  $A^-$  depend, in general, on the concentrations, thermodynamic interactions, and scattering powers of both species.<sup>21,23</sup> Clearly, both  $\Gamma^+$  and  $\Gamma^-$  depend on all four diffusion coefficients, and the general situation is rather complex. However, there are several simplifying limits. We define polymer 2 to be the relatively dilute "probe"; polymer 3 is the matrix. In this case, the needed simplifications are<sup>27</sup>

$$\lim_{c_2, c_3 \rightarrow 0} D_{23} = \lim_{c_2, c_3 \rightarrow 0} D_{32} = 0 \quad (8a)$$

$$\lim_{c_2 \rightarrow 0} D_{23} = 0 \quad (8b)$$

$$\lim_{c_2 \rightarrow 0} D_{22} = D_{22}(c_3) \approx D_{2,\text{self}}(c_3) \quad (8c)$$

Thus, if both species are very dilute, one obtains a correlation function with decay rates:

$$\Gamma^+ = q^2 D_{22}; \quad \Gamma^- = q^2 D_{33} \quad (9)$$

This permits identification of  $D_{22}$  and  $D_{33}$ . In this limit, these correspond to the mutual diffusion coefficients of species 2 and 3, respectively, in the solvent (component 1). However, as  $c_2$  and  $c_3$  are both small,  $D_{22}$  and  $D_{33}$  closely approximate the self-diffusion coefficients  $D_{2,\text{self}}$  and  $D_{3,\text{self}}$  of components 2 and 3, respectively. With appropriate hydrodynamic relationships, this permits particle sizing in bidisperse systems, provided the decays are experimentally separable.

If only the probe species (2) is dilute, one again obtains eq 9. However,  $D_{33}$  now represents a "collective" motion of the matrix, while  $D_{22}$  now approximates the self-diffusion coefficient of the probe,  $D_{2,\text{self}}(c_3)$ . If  $c_2$  is small and the matrix polymer is isorefractive with the solvent, the contribution of the  $D_{33}$  mode to the scattering is extremely weak and a single exponential decay will be observed. Though the experiments are not trivial, this ideal case has been realized in several ternary mixtures of random-coil polymers.<sup>23-25</sup> Unfortunately, miscibility becomes a very serious problem where rodlike polymers are concerned.<sup>28,29</sup> To date, our studies are limited to ternary systems in which a long rod is present at a concentration low in comparison to a chemically identical, but shorter, matrix rod. Following Davis et al.,<sup>26</sup> the strategy has been to vary the concentration of the low molecular weight matrix while holding the longer probe at constant concentration. Since it is difficult to achieve large differences in scattering power between the probe and matrix, we have, so far, maintained the concentration of the longer polymer rather high (5 mg/mL) in order to reliably observe the slow-mode diffusion corresponding to  $D_{22}$ , which should thus be considered a "particle diffusion coefficient" for the probe, a fair (but imperfect) approximation to the self-diffusion coefficient,  $D_{2,\text{self}}(c_3)$ . In what follows, we will often simply refer to the diffusion coefficient  $D_{22}$  as the "slow mode", while  $D_{33}$  is the "fast mode". These should not be confused with the same terminology as applied to concentrated binary solutions.

**Table II**  
Ternary System Studied

	molecule	$M^a$	$L$ , Å	$d$ , Å	source	$c$
probe	PBLG	210 000	1440	20	Sigma	$\leq 5$ mg/mL
matrix	PBLG	40 000	273	20	Sigma	0–120 mg/mL
solvent	DMF				Baker reagent, water $< 0.001\%$	

<sup>a</sup> From viscosity, reported by Sigma and confirmed by us. Kubota and Chu<sup>7</sup> predict that  $M_w/M_n \approx 1 + \mu_2/\bar{\Gamma}^2$  where  $\bar{\Gamma}$  and  $\mu_2$  are the first and second cumulants<sup>31</sup> of the decay profile. For our samples,  $\mu_2/\bar{\Gamma}^2 \leq 0.3$ , so we estimate  $M_w/M_n \leq 1.4$ .

Table III  
Bimodal Deconvolution of Data in Ternary Systems<sup>a</sup>

sample code	$c_3 = c_{\text{matrix}}$ , mg/mL	$c_2 = c_{\text{probe}}$ , mg/mL	$N_3 L_2^3$ <sup>b</sup>	$D_{\text{slow}}^{\text{APP}} = D_{22} \times 10^7$ , cm <sup>2</sup> /s	$D_{\text{fast}}^{\text{APP}} = D_{33} \times 10^7$ , cm <sup>2</sup> /s	$A_{\text{slow}}/A_{\text{fast}}$ ( $\pm \sim 10\%$ ), at lowest $\theta$ measured	$A_{\text{slow}}/A_{\text{fast}}$ ( $\pm \sim 10\%$ ), av over all angles measured	$c_2 M_2 / c_3 M_3$ <sup>c</sup>
P5M5	7.26	4.97	325	$1.5 \pm 0.15$	$10.3 \pm 0.8$	2.70 at $\theta = 90$		3.6
P5M10	10.2	4.72	457	$1.14 \pm 0.14$	$7.68 \pm 0.14$	2.45 at $\theta = 57.6$	2.0	2.4
P5M20	21.2	4.89	949	$1.2 \pm 0.08$	$11.1 \pm 0.2$	1.12 at $\theta = 55.05$	1.05	1.2
P5M28	27.6	4.85	1230	$1.1 \pm 0.10$	$10.6 \pm 0.9$	0.75 at $\theta = 90$		0.9
P5M50	53.7	4.74	2400	$1.2 \pm 0.03$	$12.2 \pm 0.5$	0.75 at $\theta = 55.05$	0.7	0.5
P5M80	78.2	4.66	3500	$0.66 \pm 0.07$	$11.4 \pm 0.9$	0.36 at $\theta = 90$		0.3
P5M100	96.3	4.57	4310	$0.36 \pm 0.03$	$10.5 \pm 0.38$	0.52 at $\theta = 55.05$	0.4	0.25
P5M120	120.3	4.48	5390	$0.46 \pm 0.09$	$11.5 \pm 0.2$	0.39 at $\theta = 55.05$	0.34	0.2

<sup>a</sup>  $g^{(1)}(\tau) = A_{\text{slow}} e^{-\tau/D_{\text{slow}}^{\text{APP}}} + A_{\text{fast}} e^{-\tau/D_{\text{fast}}^{\text{APP}}}$ . See also Figure 3. <sup>b</sup> This is the number of small matrix polymers in a box with volume  $L_2^3$  where  $L_2$  is the length of the probe rod. <sup>c</sup> This is the zeroth-order expectation for the ratio  $A_{\text{slow}}/A_{\text{fast}}$ , valid at  $\theta = 0$  and low concentrations.

## Experimental Section

PBLG was purchased from Sigma. Solutions were prepared by weight, and the total volume was computed by using  $v_2 = v_3 = 0.791$  mL/g and density of DMF = 0.944 g/mL. In order to reduce dust, PBLG-40, to be present at high concentrations, was first dissolved in dimethylformamide and filtered (0.2  $\mu$ m; Millipore Teflon) into deionized filtered water. The precipitate was dried under vacuum at temperatures less than 50 °C. Stock solutions of the probe polymer, PBLG-210, were prepared and filtered (0.2  $\mu$ m; Millipore Teflon) into cleaned containers, which were sealed with Teflon-faced caps and then stored in a desiccator until used to dissolve the PBLG-40 to make the ternary solutions which were finally filtered into clean fluorimeter cells (four sides polished). The resulting samples were checked for dust by observation of the scattered beam against a dark background at 100 $\times$  magnification. Minor dust was seen in some samples. However, at the flip of a lever, our detection optics permit us to see precisely the same volume that will be measured by the phototube. In all the samples reported, the frequency of dust in this small volume was very low. Indeed, most samples were sufficiently clean for automatic data collection. However, in some instances the correlator was operated manually while sudden deflections of a ratemeter, indicating scattered intensity, were watched for. When such deflections were seen, the entire run was discarded.

The home-built spectrometer employed a 7-mW HeNe laser operating at 6328 Å (Hughes), which was sufficient for these studies when focused with a 6-cm lens. A few experiments were performed by using a Lexel Model 95 argon ion laser (2 W at 5145 Å). The results from either laser were identical. The phototube was a Hamamatsu R928P, selected for photon counting, that was connected to a Pacific Precision Instruments Model AD126 photon counting system. There was no correlated afterpulsing beyond 1  $\mu$ s. The correlator was a 144-channel Langley Ford Model 1096, equipped with 80-channel "multi- $\tau$ " option, enabling three simultaneous correlation functions to be obtained at different channel times using the same photopulses. For the first correlation function, the instrument acted as a 4-bit correlator, while the capacity of the shift registers was increased for the higher correlation functions to prevent saturation (overflow). This device was invaluable in the present study, since correlation functions that spanned the interesting range could be obtained without any artificial device, such as splicing. It was always possible to assign a sufficient number of channels to a time-delay region where the correlation function was actively decaying. Instrument control and data analysis were performed with an IBM PC-XT computer equipped with an Intel 8087 80-bit math coprocessor. At each angle and concentration, a number (typically 15) of correlation functions were obtained, and each was analyzed by a second-order cumulants<sup>30</sup> fit. Abnormal runs were rejected. The factors identifying a run as abnormal are discussed in ref 1. The remaining runs were summed to give a net correlation function with base line typically  $10^6$ – $10^7$ , and this was refitted using first-, second-, and third-order cumulants. Next, a discreet multiple exponential nonlinear least squares algorithm was applied to the summed data. Though the routine will handle up to five exponentials, we used only a bimodal analysis, as appropriate to the problem at hand. The use of correlation functions with small base lines (in this case corresponding to total data acquisition periods of about 5–30 min) is justified by the wide separation of the decay

rates. In general, we recommend higher quality data (e.g., base lines of  $10^6$ ), particularly if the decay rates are separated by a factor of 3 or less or if one component is minor. All experiments were at 40 °C.

## Results and Discussion

A typical correlation function is shown in Figure 1. The bimodal nature of the decay is clearly evident from the semilogarithmic representation (Figure 1c). Even without fitting the data by computer, it was possible to see that the slow mode became increasingly slow as matrix concentration was increased, while the fast mode increased slightly. Figure 2 shows the angular dependence for both fast and slow decays at two disparate concentrations; each appears linear in  $q^2$ . The concentration dependences of slow and fast modes are reported in Table III and plotted in Figure 3. Errors were estimated empirically by measuring the effects of time window (the range of delay times covered) and base-line uncertainty on several of the samples. The statistical uncertainty from the fitting algorithm is much less. In all cases, the multiexponential algorithm was very insensitive to initial guess, and fitted base lines typically agreed with the theoretical base line to within 0.1%. Generally, two exponentials were sufficient to fit  $g^{(1)}(\tau)$  to within statistical uncertainty. Failure of the two-exponential approach was never severe. (Mean-square residual divided by uncertainty in measurements,  $\chi^2$ , was  $\sim 7$  in the worst case. However, better data with less uncertainty would increase the value of  $\chi^2$ .) We attribute this degree of failure to a small amount of polydispersity and also an additional slow mode arising from the matrix, as is now expected in many concentrated polymer solutions (see ref 16–19 and citations therein). Correlation functions measured with the matrix polymer alone showed a very weak slow-mode decay. Whether this additional slow contribution comes from the finite rod cross section, as suggested in ref 14, or from coupled rotational-translational motions, valid even for infinitely thin rods, is unknown. The effect of an additional very slow decay would be to decrease the estimate for slow-mode diffusion. The good agreement between fitted and theoretical base lines indicates that this effect is minor.

Because of the substantial experimental uncertainties, the precise dependence of  $D_{\text{slow}}^{\text{APP}}$  on  $c_3$  cannot be established. Thus, even though the plateau near  $0.5D^0$  is very intriguing, the solid curve in Figure 3 is merely to guide the eye. It is especially difficult to trace the initial rapid decline in  $D_{\text{slow}}^{\text{APP}}$ . The problem is that as the matrix concentration,  $c_3$ , decreases, the double-exponential fit responds increasingly to the small polydispersity of the larger probe polymer. The severity of this problem can be gauged from the ratio of scattering intensities of the two modes,  $A_{\text{slow}}/A_{\text{fast}}$ . We are not aware of any theory predicting  $A_{\text{slow}}/A_{\text{fast}}$  for semiflexible rods in concentrated

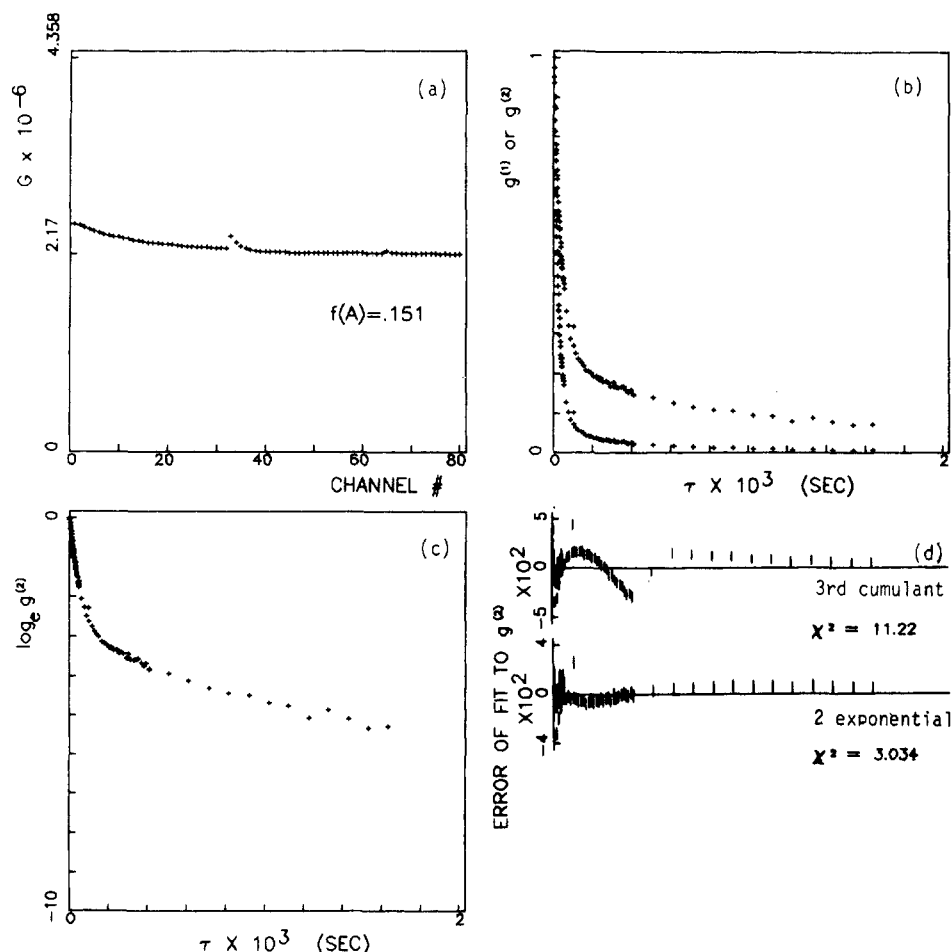


**Figure 1.** Correlation function, in several representations, for ternary solution P5M120: PBLG-210 (probe) at 4.5 mg/mL; PBLG-40 (matrix) at 120.3 mg/mL; DMF at 40 °C;  $\theta = 60.4^\circ$  ( $qL_{\text{probe}} \approx 2$ ); acquisition time = 3000 s as 16 separate runs;  $\lambda_0 = 6328 \text{ \AA}$ . (a) Raw data counts for homodyne correlation function.  $G(\tau) = B(1 + f(A)|g^{(1)}(\tau)|^2)$  where  $B$  = base line,  $f(A)$  = coherence factor. Due to memory limitations, our 144-channel correlator only gives 80 channels in the "multi- $\tau$ " mode. The three correlation functions shown overlap at short times and were measured simultaneously at  $\Delta\tau = 1.6, 12.8$ , and  $102.4 \mu\text{s}$ , channels 1–32, 33–64, and 64–80, respectively. The instrument is capable of much higher  $f(A)$ , but the optics were adjusted to optimize ease of data collection with our relatively weak He–Ne laser. (b) Normalized, base-line-subtracted correlation functions  $g^{(1)}(\tau)$  (upper curve) and  $g^{(2)}(\tau) = |g^{(1)}(\tau)|^2$  (lower curve). (c) Semilog representation of  $g^{(2)}(\tau)$  showing the bimodal character of the decay. (d) Error plots for third-cumulant fit and double-exponential fit. The horizontal (time) scale is the same as in b. Vertical distance from 0 line to center of a bar is the error of fit for a given channel. The height of each bar represents the uncertainty in measurement of  $g^{(2)}(\tau)$  and is the same for both fits. (Note scale expansion in double-exponential fit.) If all bars touch the line of 0 error, the data is fit to within statistical uncertainty:  $\chi^2 = 1$ .

ternary solution. However, for the relatively dilute solutions, a zeroth-order expectation is  $A_{\text{slow}}/A_{\text{fast}} \approx P_2(qL_2)c_2M_2/c_3M_3$  where  $P_2(qL_2)$  is the particle form factor for the longer (probe) rod. (In the present experiments the particle form factor for the shorter rod,  $P_3(qL_3)$ , is near unity 1 at all  $q$ .) If this is true,  $P_2(qL_2) = (A_{\text{slow}}/A_{\text{fast}})/(c_2M_2/c_3M_3)$  should roughly equal the theoretical  $P_2(qL_2)$  (see tables of ref 31). Figure 4 and Table III show that for  $7 \leq c_3 \leq 28 \text{ mg/mL}$  adherence to this admittedly simple expectation is well within experimental uncertainty. Below 7 mg/mL, serious deviations were noted and were attributed to the polydispersity problem just described. The slow component became relatively stronger at  $c_3 > 50 \text{ mg/mL}$ , although the angular dependence was not markedly altered, within experimental uncertainty, suggesting freedom from aggregation or dust, and Figure 1 shows that the correlation function is still clearly separated into two decay modes.

Despite the uncertainties, the decrease in slow-mode apparent diffusion clearly meets or exceeds the Doi–Edwards prediction for an infinitely stiff, infinitely thin rigid rod. While the magnitude of decrease is mild in comparison to ref 14, it is comparable to that obtained for binary solutions after thermodynamic correction in ref 1.

This qualitative agreement has encouraged us to plot the data from ref 1 in the fashion suggested by eq 4. See Figure 5. The four points at concentrations in excess of  $(dL^2)^{-1}$  do appear to fall on a straight line, with intercept somewhat below the predicted  $D^0/2$ . The slope gives a value of  $g \approx 0.02$ , much less than expected for a perfectly rigid rod. The implications of this result are threefold:

(1) The low intercept may be explained as the extra friction of the bent rod, compared to a rigid one, for motion in a direction parallel to its nominal axis through a complex matrix of other polymers. It is unclear whether this value represents the true translational anisotropy of the bent rod in dilute solution, since the extrapolation is made from a regime where the friction arises partly from polymer–polymer interaction.

(2) In contrast, because it is only bent temporarily, the semiflexible rod can jump over the "gates" placed in its path by neighbors of finite diameter, and this may account for the very low  $g$  value. Whatever the reason, a low  $g$  value is qualitatively consistent with the high  $\beta^{1/2}$  values noted previously.

(3) Due to low  $g$  and high  $\beta^{1/2}$  values, the "glass" state envisioned by Edwards and Evans may indeed be unrealizable in the equilibrium isotropic state. However, a

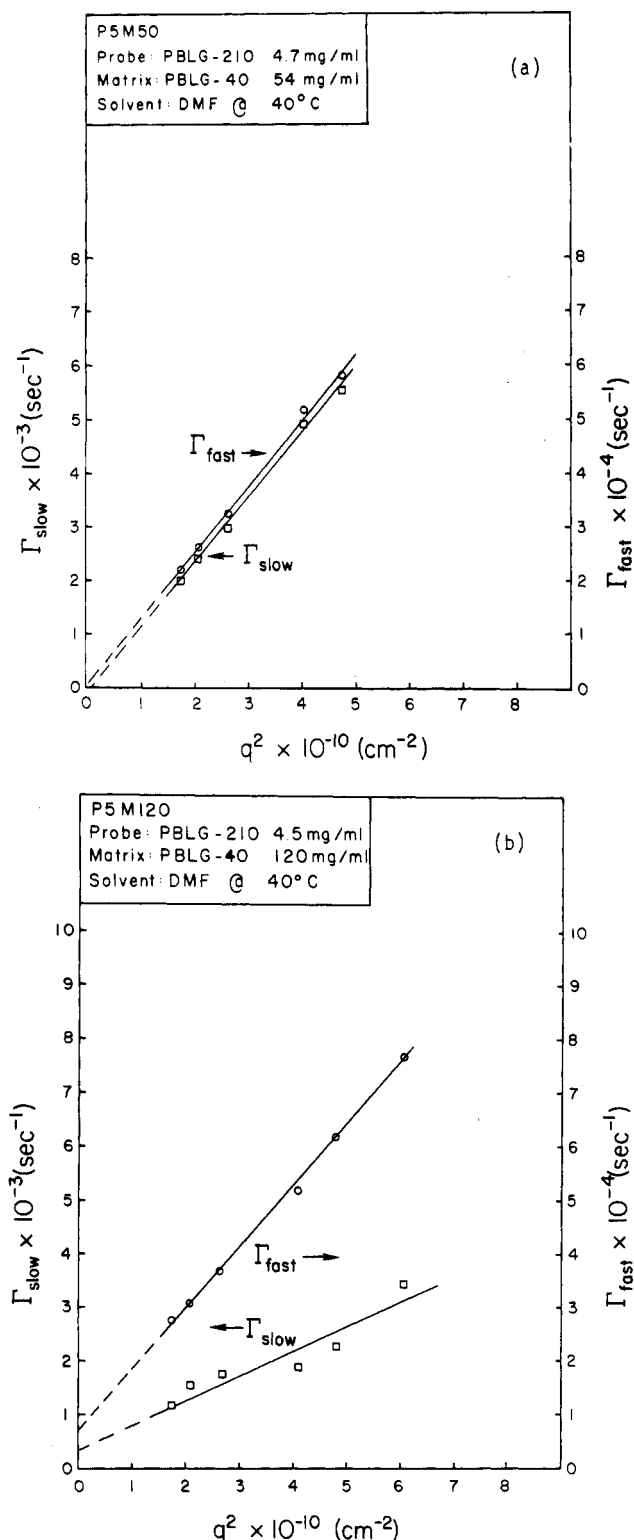


**Figure 2.** Angular dependence of fast (○) and slow (□) exponential decay rates for probe (PBLG-210) concentrations of about 4.5 mg/mL: (a) matrix (PBLG-40) concentration = 54 mg/mL; (b) matrix (PBLG-40) concentration = 120 mg/mL. The slope for the fast mode is similar at both concentrations, while the slow-mode is much less in b.

metastable frozen state might be achievable by rapidly quenching a rodlike polymer solution into its wide biphasic region. In the emerging polymer-rich phase, frozen, essentially isotropic (or poorly ordered) bundles of the polymer at high concentration may be created, at least over microscopic domains, before liquid crystalline structure can form. In this regard, it is interesting to note that rodlike polymers without visible means of cross-linking

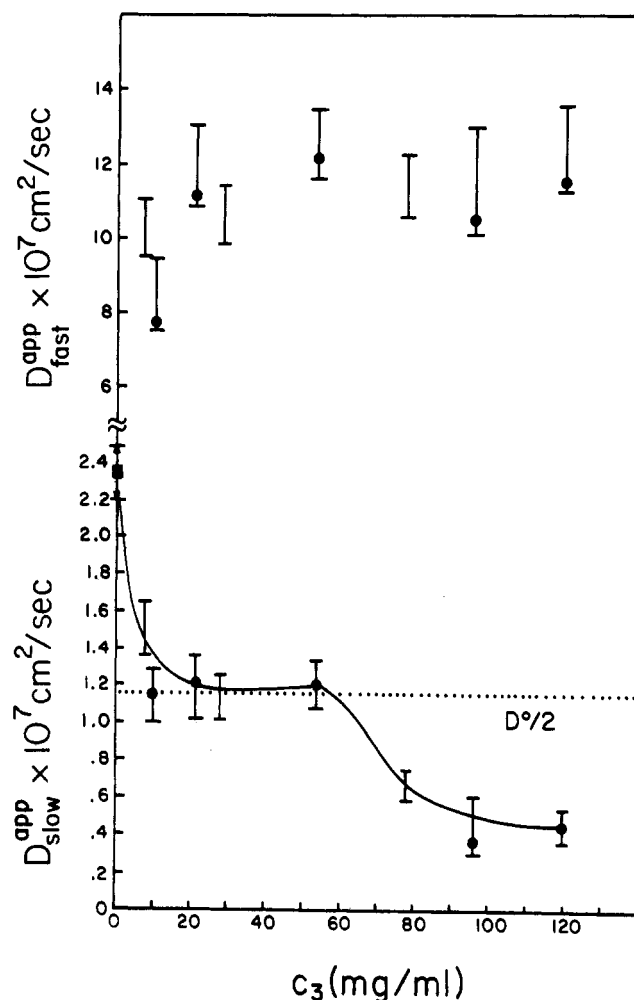


**Figure 3.** Dependence of apparent diffusion coefficients of slow and fast modes on matrix polymer concentration,  $c_3$ . For points with filled circles  $D$  is calculated as  $d\Gamma/dq^2$ . Otherwise,  $D$  is taken as  $(\Gamma/q^2)_{q=90^\circ}$ . The point at  $c_3 = 0$  (■) represents a cumulant fit for the binary solution PBLG-210 at 5 mg/mL in DMF, but a single-exponential fit lies within the stated error bars for this point. See also Table III and text for discussion of error bars.

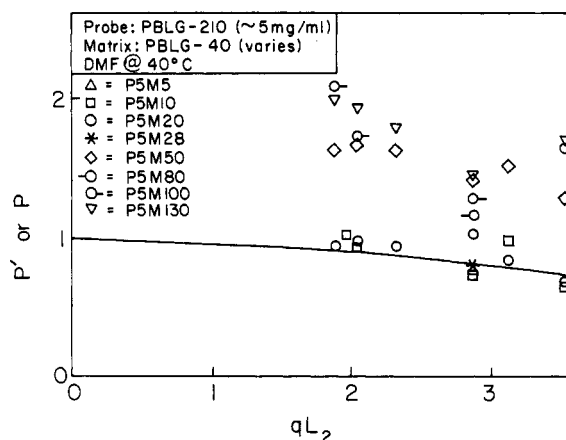


**Figure 4.**  $P_2'(qL_2) = (A_{\text{slow}}/A_{\text{fast}})/(c_2M_2/c_3M_3)$  and the theoretical form factor  $P_2(qL_2)$ . Agreement at moderate  $c_3$  is within experimental uncertainty ( $\approx 10\%$ ), while amplitude of the probe component (2) increases at higher  $c_3$ .

have been observed to gel reversibly under such treatment.<sup>32,33</sup>

For PBLG, the emerging picture is one in which the onset of entanglement behavior in binary solutions occurs at a concentration higher than expected for rigid rods. However, entanglement ultimately reduces the transla-

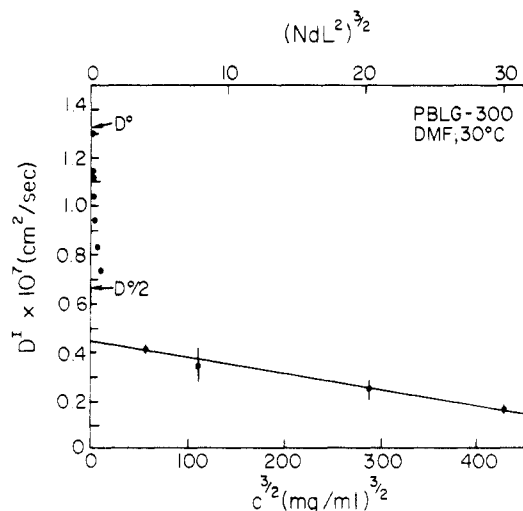


**Figure 5.** Data of ref 1 for binary solutions of PBLG-300 ( $M = 300\,000$ ) plotted in the format suggested by eq 4.  $D^1$  is an approximation to the self-diffusion coefficient obtained by making a thermodynamic correction, as discussed in ref 1. The linear correlation coefficient of the four data points for which  $NdL^2 > 1$  was 0.9995.

tional diffusion coefficient more than expected for a perfectly rigid, infinitely thin rod, but less than expected for a perfectly rigid rod of finite thickness. This behavior may be explained, in part, by hypothesizing the wiggling of the rodlike polymer. Flexural motion relaxes entanglements of a very local nature, but results in a larger instantaneous cross section for motions parallel to the nominal axis than a perfectly rigid rod would have, thus introducing barriers to diffusion along the axis of any rod, even an infinitely thin one. However, these barriers are "soft", meaning that they can be relaxed by the very flexural motions that cause them, which is also true of barriers due to finite thickness.

## Conclusion

Dynamic light scattering has been used to follow the motion of a large rodlike polymer at relatively low concentration in a matrix made up of chemically identical small rodlike polymers. The correlation functions are fit well by two exponentials over a wide range of matrix concentration. The slow-mode decay is associated with the "particle diffusion coefficient",  $D_{22}$ , of the larger rod through the complex matrix, and this should be close to the true self-diffusion coefficient of the larger rod.  $D_{22}$  is found to decrease by as much or more than predicted in the Doi-Edwards theory for perfectly rigid, infinitely thin rods. The magnitude of decrease is substantially less than found by identifying the slow mode of concentrated binary solutions of poly(*n*-butyl isocyanate) in  $\text{CCl}_4$  with the self-diffusion of the rigid rod but is comparable to earlier estimates of self-diffusion in binary solution, which relied on an approximate thermodynamic correction. When these older data are analyzed in accordance with the Evans-Edwards equation, the serious effects of rod flexibility are again suggested, but a linear plot does result at suf-

ficiently high concentration.

**Acknowledgment.** I am grateful to the donors of the Petroleum Research Fund, administered by the American Chemical Society, and to the Cottrell Program at Research Corp. for support of this work.

**Registry No.** PBLG (homopolymer), 25014-27-1; PBLG (SRU), 25038-53-3.

## References and Notes

- (1) Russo, P. S.; Langley, K. H.; Karasz, F. E. *J. Chem. Phys.* **1984**, *80*, 5312.
- (2) (a) Doi, M.; Edwards, S. F. *J. Chem. Soc., Faraday Trans. 2* **1978**, *74*, 560. (b) Doi, M.; Edwards, S. F. *J. Chem. Soc., Faraday Trans. 2* **1978**, *74*, 918.
- (3) Jamieson, A. M.; Southwick, J. G.; Blackwell, J. J. *Polym. Sci., Polym. Phys. Ed.* **1982**, *20*, 1513.
- (4) Zero, K. M.; Pecora, R. *Macromolecules* **1982**, *15*, 87.
- (5) Matheson, R. R., Jr. *Macromolecules* **1980**, *13*, 643.
- (6) Odell, J. A.; Atkins, E. D. T.; Keller, A. *J. Polym. Sci., Polym. Lett. Ed.* **1983**, *21*, 289.
- (7) Kubota, K.; Chu, B. *Biopolymers* **1983**, *22*, 1461.
- (8) (a) Keep, G.; Pecora, R. *Macromolecules* **1985**, *18*, 1167. (b) Maeda, T.; Fujime, S. *Macromolecules* **1984**, *17*, 2381.
- (9) Thomas, J. C.; Fletcher, G. C. *Biopolymers* **1979**, *18*, 1333.
- (10) Ostrowski, N.; Sornette, D.; Parker, P.; Pike, E. *Opt. Acta* **1981**, *28*, 1059.
- (11) (a) Powers, J.; Peticolas, W. In "Ordered Fluids and Liquid Crystals"; Johnson, J.; Porter, R. S., Eds.; American Chemical Society: Washington, DC, 1967; ACS Adv. Chem. Ser., No. 63, p 217. (b) Kihara, H. *Polym. J.* **1975**, *7*, 406. (c) Boeckel, G.; Genzling, J.; Weill, G.; Benoit, H. *J. Chim. Phys.* **1962**, *59*, 999. (d) Elias, H.; Gerber, J. *Makromol. Chem.* **1968**, *112*, 142.
- (12) Edwards, S. F.; Evans, K. E. *J. Chem. Soc., Faraday Trans. 2* **1982**, *78*, 113.
- (13) Statman, D.; Chu, B. *Macromolecules* **1984**, *17*, 1537.
- (14) Ambler, M. R.; McIntyre, D.; Fetters, L. J. *Macromolecules* **1978**, *11*, 300.
- (15) (a) Tsutsumi, A.; Hikichi, K.; Kaneko, M. *Rep. Prog. Polym. Phys. Jpn.* **1970**, *13*, 331. (b) Saba, R. G.; Sauer, J. A.; Woodward, A. E. *J. Polym. Sci., Part A* **1963**, *1*, 1483. (c) Koleske, J. V.; Lundberg, R. S. *Macromolecules* **1969**, *2*, 438. (d) Hiltner, A.; Anderson, J. M.; Borkowski, E. *Macromolecules* **1972**, *5*, 446. (e) Tschoegel, N. W.; Ferry, J. J. *Am. Chem. Soc.* **1964**, *86*, 1474. (f) Iwata, K. *Biopolymers* **1980**, *19*, 125. (g) Schmidt, M. *Macromolecules* **1984**, *17*, 553.
- (16) Tirrell, M. *Rubber Chem. Technol.* **1984**, *57*, 523.
- (17) Brown, W.; Johnson, R. M.; Stilbs, P. *Polym. Bull. (Berlin)* **1983**, *9*, 305.
- (18) Chang, T.; Yu, H. *Macromolecules* **1984**, *17*, 115.
- (19) Nemoto, N.; Makita, Y.; Tsunashima, Y.; Kurata, M. *Macromolecules* **1984**, *17*, 2629.
- (20) Phillies, G. D. J. *J. Chem. Phys.* **1974**, *60*, 983.
- (21) Pusey, P. N.; Fijnaut, H. M.; Vrij, A. *J. Chem. Phys.* **1982**, *77*, 4270.
- (22) Hanley, B.; Balloge, S.; Tirrell, M. *Chem. Eng. Commun.* **1983**, *24*, 93.
- (23) Lodge, T. *Macromolecules* **1983**, *16*, 1393.
- (24) Martin, J. E. *Macromolecules* **1984**, *17*, 1279.
- (25) Davis, P.; Snook, I.; van Megen, W.; Preston, B. N.; Comper, W. D. *Macromolecules* **1984**, *17*, 2376.
- (26) Vitagliano, V.; Sartorio, R. *J. Phys. Chem.* **1970**, *74*, 2949.
- (27) Flory, P. J. *Macromolecules* **1978**, *11*, 1138.
- (28) Gupta, A. K.; Benoit, H.; Marchal, E. *Eur. Polym. J.* **1979**, *15*, 285.
- (29) Koppel, D. E. *J. Chem. Phys.* **1972**, *57*, 4814.
- (30) Kratochvil, P. In "Light Scattering From Polymer Solutions"; Huglin, M. B., Ed.; Academic Press: New York, 1972.
- (31) Tohyama, K.; Miller, W. G. *Nature (London)* **1981**, *289*, 813.
- (32) Sasaki, S.; Hikata, M.; Shiraki, C.; Uematsu, I. *Polym. J.* **1982**, *14*, 205.